

Ab Initio Molecular Dynamics Simulation of Liquid $\text{Ga}_x\text{As}_{1-x}$ Alloys

R. V. Kulkarni and D. Stroud

Department of Physics, The Ohio State University, Columbus, Ohio 43210

(April 26, 2024)

Abstract

We report the results of *ab initio* molecular dynamics simulations of liquid $\text{Ga}_x\text{As}_{1-x}$ alloys at five different concentrations, at a temperature of 1600 K, just above the melting point of GaAs. The liquid is predicted to be metallic at all concentrations between $x = 0.2$ and $x = 0.8$, with a weak resistivity maximum near $x = 0.5$, consistent with the Faber-Ziman expression. The electronic density of states is finite at the Fermi energy for all concentrations; there is, however, a significant pseudogap especially in the As-rich samples. The Ga-rich density of states more closely resembles that of a free-electron metal. The partial structure factors show only a weak indication of chemical short-range order. There is also some residue of the covalent bonding found in the solid, which shows up in the bond-angle distribution functions of the liquid state. Finally, the atomic diffusion coefficients at 1600K are calculated to be $2.1 \times 10^{-4} \text{ cm}^2/\text{sec}$ for Ga ions in $\text{Ga}_{0.8}\text{As}_{0.2}$ and $1.7 \times 10^{-4} \text{ cm}^2/\text{sec}$ for As ions in $\text{Ga}_{0.2}\text{As}_{0.8}$.

I. INTRODUCTION

The study of liquid metals and alloys has drawn considerable attention recently, in particular due to the possibility of carrying out first principles or *ab initio* calculations for these systems. In these calculations the electronic structure is evaluated quantum mechanically using Density Functional Theory (DFT) and the corresponding forces are used to move the ions according to classical molecular dynamics. Using this approach it is possible to calculate both the atomic and electronic structure consistently and to see how changes in one are correlated with changes in the other. By now, a number of groups have used these methods to calculate both the thermodynamic and transport properties of a variety of liquid metals and alloys [1–3].

Liquid semiconductors are of particular interest from the point of view of *ab initio* calculations. By “liquid semiconductors,” we mean liquids of materials which are semiconducting in their *solid* phases, such as Si, Ge, GaAs, and CdTe. Somewhat surprisingly, most of these are reasonably good metals in their *liquid* phases. For example, Si, Ge, and GaAs all have conductivities near melting which lie in the metallic range, and which tend to decrease with increasing temperatures, as is characteristic of metals. This metallic behavior is correlated with an increase in coordination number on melting, the liquid is thus more close-packed than the solid and has a higher density. By contrast, ℓ -CdTe is poorly conducting in its liquid state and its conductivity *increases* with increasing temperature, characteristic of semiconductors.

Recent *ab initio* calculations for several of these materials give behavior which is in good agreement with these experiments. Godlevsky *et al* [4] have found, in agreement with experiment, that stoichiometric GaAs is metallic, whereas stoichiometric CdTe is a reasonable insulator. These differences in the electronic properties were related to the differences in the structural properties occurring within the melt. An earlier calculation by Zhang *et al* [5] studied stoichiometric ℓ -GaAs using the Car-Parrinello version of *ab initio* molecular dynamics [6,7]. In this calculation too, it was found that ℓ -GaAs is a metallic, weakly ionic

liquid, with a larger coordination number than the insulating solid phase.

In this paper, we describe a numerical study of $\ell\text{-Ga}_x\text{As}_{1-x}$ over a range of concentrations, using *ab initio* techniques. The liquid is miscible over the whole concentration range, unlike the solid, which exists only at stoichiometry. Such a study is of interest for a variety of reasons. The properties of $\ell\text{-Ga}$ and $\ell\text{-As}$ stand in marked contrast to each other. $\ell\text{-Ga}$ is a close-packed liquid metal with a coordination number of ~ 9 and its electronic density of states is almost free-electron like. In contrast, $\ell\text{-As}$ has the same coordination number as in the crystalline phase (~ 3), and is a narrow band-gap semiconductor in the liquid state. Thus while we expect $\ell\text{-Ga}$ to show metallic bonding, $\ell\text{-As}$ is expected to retain the covalent character of the bond upon melting. Previous *ab initio* calculations for these liquids [8,2] have indeed confirmed this picture. Thus as the stoichiometry is varied for $\ell\text{-Ga}_x\text{As}_{1-x}$, we would expect interesting changes both structurally and electronically. It is also of interest to compare the structures of $\ell\text{-Ga}_x\text{As}_{1-x}$ for $x = 0.2$ and $x = 0.8$ with the structure for the corresponding pure liquids (As and Ga respectively) to see how changes in structural properties are correlated with changes in electronic properties.

We turn now to the body of the paper. In section II, we briefly summarize our approach and method of calculation. Our results are presented extensively in Section III, together with some analysis connecting the calculations to a qualitative picture of the liquid state. Finally, in Section IV, we give a short concluding discussion.

II. METHOD AND COMPUTATIONAL DETAILS

Our method of carrying out the *ab initio* simulations is similar to that of our previous work [9,10]. We use the plane-wave pseudopotential approach with generalized norm-conserving pseudopotentials [11] in the Kleinman-Bylander form [12], treating the *d*-wave part as the local component. The exchange-correlation potential is computed using the local-density approximation (LDA), using the Ceperley-Alder result for the exchange-correlation energy, as parametrized by Perdew and Zunger [13]. The details of the code can be found

in the literature [14,15]

Our liquid-state molecular dynamics (MD) simulations were carried out at a temperature $T = 1600$ K [20], just above the melting point of GaAs ($T = 1515$ K). We have considered five concentrations of $\text{Ga}_x\text{As}_{1-x}$: $x = 0.2, 0.4, 0.5, 0.6$, and 0.8 . In each case, we used a cubic 64-atom supercell with periodic boundary conditions. For this size cell, the actual numbers of Ga atoms in the five samples were 13, 26, 32, 38, and 51. (Since the minority component in the 20% and 80% samples, the statistics will be quite poor for them and the results should be given greatest significance for the majority components in those cases.) The atomic densities for the five concentrations were obtained from the measured density of ℓ -GaAs at this temperature [17], together with Vegard's Law (i. e. linear interpolation of atomic volumes) [18]. We use a 10-Ry cutoff for the energies of the plane waves included in the wave function expansion, and Γ -point sampling for the supercell Brillouin zone. For the electronic structure, we used Fermi-surface broadening corresponding to an electronic subsystem temperature of $k_B T^{el} = 0.1\text{eV}$. In calculating the electronic wave functions, at each concentration we include eight empty bands. We control the ionic temperature using the Nosé-Hoover thermostat [19]. The equations of motion are integrated by means of the Verlet algorithm, using an ionic time step of 125 a.u. (~ 3 fs). For each concentration, the samples were equilibrated for about 0.2ps, following which simulations were carried out for more than 3ps.

These simulations start from an initial configuration which, for the stoichiometric liquid, was generated from a classical molecular-dynamics (CMD) simulation using potentials of the Stillinger-Weber form. Although our particular potentials were originally derived for liquid $\text{Ge}_x\text{Si}_{1-x}$ alloys, they should give a reasonable *starting* configuration for the $\text{Ga}_{1-x}\text{As}_x$ alloys which we study. We use these potentials but with Ga and As masses rather than those of Si and Ge. This model system was melted using classical molecular dynamics at high temperatures, then cooled down gradually to the temperature of interest. The configuration thus obtained from CMD was equilibrated for 0.2 ps (about double the expected relaxation time for this system). For the nonstoichiometric liquids, we used the same starting configuration

as in the stoichiometric case, but with Ga atoms randomly substituted for the appropriate number of As atoms (or vice versa), so as to give the correct concentration.

III. RESULTS

Fig. 1 shows the three partial pair correlation functions $g_{GaGa}(r)$, $g_{AsAs}(r)$ and g_{GaAs} for liquid Ge_xAs_{1-x} at the concentration $x = 0.5$ and a temperature $T = 1600$ K. A number of features deserve mention. First, at $x = 0.5$, the principal peaks of all three partial pair correlation functions occur at about the same separation, namely 2.5\AA . This indicates the non-ionic character of the bonds; in ionic liquids the partial pair correlation functions for like atoms are out of phase with the corresponding function for unlike atoms [21]. Our results for $g_{\alpha\beta}(r)$ are in close agreement with the recent calculation by Godlevsky *et al* [4]; an earlier calculation by Zhang *et al* [5] also gives the same features although these authors get a much stronger principal peak for $g_{GaAs}(r)$ than is found in either our calculations of that of Ref. [4]. While the principal peaks are in phase, there are some differences among the partial $g(r)$'s. For example, at $x = 0.5$, $g_{AsAs}(r)$ has a slightly higher and narrower first peak, and a stronger second peak, than $g_{GaGa}(r)$, while $g_{GaGa}(r)$ has a broad first peak and no obvious peak beyond that. We have also calculated the coordination numbers for the first shell of neighbors, defined as the integral of $4\pi\rho r^2 g(r)$ from zero out to the minimum after the first maximum in $g(r)$. [Here $g(r)$ is the *total* pair correlation function, which does not distinguish between the two species, normalized so that it approaches unity at large r .] The coordination we calculate in this way at $T = 1600$ K is 5.8, in good agreement with the experimental estimate of 5.5 ± 0.5 . Note also that this value is larger than the diamond-structure value of 4 but significantly smaller than the value expected in a close-packed liquid, which would be in the range of 9 or 10. This value indicates the persistence of covalent bonding in ℓ -GaAs.

Fig. 2 shows $g_{GaGa}(r)$ at $x = 0.8$ and $g_{AsAs}(r)$ at $x = 0.2$. The latter shows more short-range order than the former - specifically, a sharper main peak and a broad second peak, rather than a single broad principal peak. We believe that there are several causes for these

differences. First, pure Ga has a much lower melting temperature than either $\text{Ga}_{0.5}\text{As}_{0.5}$ or As. Thus, at the same temperature of 1600 K, we expect less short-range order for $g_{\text{GaGa}}(r)$ at $x = 0.8$ than for $g_{\text{AsAs}}(r)$ at $x = 0.2$, as seen in our calculations. In addition, we expect the $x = 0.2$ sample to show some residue of the complex local structure seen in pure ℓ -As, which is, in turn, quite similar to that of the crystalline phase [8,22]. Indeed, our calculated $g_{\text{AsAs}}(r)$ at $x = 0.2$ has some of the same features as those in the calculated $g(r)$ for pure ℓ -As [8]. However, there are also some observable differences, which may be related to the fact that, experimentally, pure ℓ -As is semiconducting [22] while $\ell\text{-Ga}_{0.2}\text{As}_{0.8}$ is calculated to be metallic (as shown later when we calculate the electronic structure). First, if we integrate $g_{\text{AsAs}}(r)$ for the $x = 0.2$ sample out to the first minimum beyond the main peak, we obtain a coordination number of 3.2 As atoms for the first shell of nearest neighbors surrounding an As atom. This is slightly larger than the value 3 reported for pure ℓ -As (at $T=1150$ K) experimentally and in previous calculations [8,23]. A more important difference is that pure ℓ -As has a sharp second peak in $g(r)$ [22], whereas for $g_{\text{AsAs}}(r)$ in our simulations this second peak is very broad. While some of this broadening may result from the higher temperature ($T = 1600$ K) in our simulations for $x = 0.2$, these results suggest that the local structure seen in ℓ -As is preserved *only* out to the first shell of neighbors in $\ell\text{-Ga}_{0.2}\text{As}_{0.8}$.

On the other hand, the features we see for $g_{\text{GaGa}}(r)$ at $x = 0.8$ are qualitatively similar and consistent with those seen for liquid Ga at lower temperatures [2,26]. Using the procedure indicated above, we get a Ga coordination number of 5.8 for the first shell. If we integrate the total $g(r)$ up to the first shell (i. e., including both As and Ga neighbors of Ga), we obtain a Ga coordination number of 6.9. While these values are smaller than the coordination number of 9.0 reported for pure ℓ -Ga [26], we attribute the difference to the lowering of the first peak due to the higher temperature of our simulations ($T = 1600$ K) compared to those for pure ℓ -Ga ($T = 702$ K and $T = 982$ K) [2].

Figs. 3-5 show information about the various partial alloy structure factors at the same temperature. The partial structure factors $S_{ij}(\mathbf{k})$ are defined in one of the standard ways [24,25]:

$$S_{ij}(\mathbf{k}) = (N_i N_j)^{-1/2} \left\langle \sum_i \sum_j e^{-i\mathbf{k} \cdot (\mathbf{R}_i - \mathbf{R}_j)} \right\rangle - (N_i N_j)^{-1/2} \delta_{\mathbf{k},0} \quad (1)$$

where i and j denote the two components of the binary alloy. Fig. 3 shows the calculated total structure factor $S(\mathbf{k})$, as weighted by neutron scattering factors at a concentration $x = 0.5$. $S(\mathbf{k})$ is defined by

$$S(k) = \frac{b_i^2 S_{ii}(k) + 2b_i b_j S_{ij}(k) + b_j^2 S_{jj}(k)}{b_i^2 + b_j^2} \quad (2)$$

where b_i and b_j are the corresponding experimental neutron-scattering lengths ($b_{Ga} = 7.2$ and $b_{As} = 6.7$) For comparison, we also show in Fig. 3 the quantity $S(\mathbf{k})$ as measured by neutron diffraction [27]. As can be seen from the Figure, the two agree quite well. In particular, the calculations convincingly reproduce the experimentally observed shoulder on the high- k side of the principal peak in $S(\mathbf{k})$.

Fig. 4 shows the three partial alloy structure factors $S_{GaGa}(\mathbf{k})$, $S_{AsAs}(\mathbf{k})$, and $S_{GaAs}(\mathbf{k})$ at $x = 0.5$ and $T = 1600\text{K}$. The structure factor for like pairs is always positive, with a conspicuous first peak, while the structure factor between opposite pairs is negative for small k , becoming positive at k values corresponding to the peaks in the other two partial structure factors. It is of interest to compare these results to those found in other model calculations. For a mixture of hard spheres of packing fraction 0.45 (characteristic of the liquid near melting) and ratio of hard sphere diameters of 0.9 [28], the cross-correlation function is negative at small k and has a peak near that of the two same-species functions, as in our calculations. By contrast, for liquid NaCl, which is strongly ionic, the cross-correlation function has a strong *negative* peak at the same k as the peaks of the same-species partial structure factors. Thus, our results are more similar to the hard-sphere structure factors, suggesting that liquid GaAs is at most only weakly ionic.

Finally, Fig. 5 shows $S_{GaGa}(\mathbf{k})$ at $x = 0.8$ and $S_{AsAs}(\mathbf{k})$ at $x = 0.2$. Once again, like the real-space correlation functions at the same concentrations, the Ga-Ga structure factors show slightly less correlation (i. e., a lower principal peak and a less conspicuous second peak) than do the corresponding As-As structure factors. One possible reason for this behavior, as

for the corresponding real-space correlation functions, is that the $x = 0.8$ sample is further from melting than is the $x = 0.2$ liquid.

$S_{AsAs}(k)$ for $x = 0.2$ shows characteristic differences from that for pure ℓ -As, which are analogous to those discussed earlier for the $g(r)$'s. Specifically, $S(k)$ for pure ℓ -As [22] has a split principal peak with maxima at $k = 2.45 \text{ \AA}^{-1}$ and $k = 3.74 \text{ \AA}^{-1}$. By contrast, $S_{AsAs}(k)$ for $x = 0.2$ has a peak at 2.5 \AA , but the second peak is reduced to only a shoulder at about 3.5 \AA . The fact that the second of the split peaks is smoothed to a shoulder at $x = 0.2$ indicates a change in the local structure which is also reflected in the reduction of the second peak of partial $g(r)$ as noted earlier.

We next discuss the $x = 0.8$ sample, comparing our results with those for pure ℓ -Ga at lower temperatures [2,26]. The partial structure factor show the same qualitative features as the structure factors for the pure liquid, but there are some quantitative differences. Our results for $x = 0.8$ (at 1600 K) show a first peak in $S_{GaGa}(k)$ with a maximum of only about 1.3, which is lower than the experimental one seen in pure Ga at 959 K (~ 1.7). We attribute the lowering of the first peak to the increased temperature, as seen experimentally in most liquid metals.

Further information about the short-range order in the liquid alloy may be obtained from *bond angle distribution functions*, shown in Figs. 6 and 7. These functions are defined by analogy with our previous work in liquid Ge [9,10]. Namely, one considers a group of three atoms. Of these, one is denoted as the central atom; the other two atoms (denoted as “side atoms”), with the central atom, define a bond angle θ . $g_3(\theta, r_c)$ is the distribution of bond angles formed by all such groups of three atoms, such that both the side atoms lie within a cutoff distance r_c of the central atom. Fig. 6 shows $g_3(\theta, r_c)$ for the Ga-Ga-Ga angles at $x = 0.8$, and for the As-As-As angles at $x = 0.2$, each for two different choices of the cutoff radius r_c . Fig. 7 shows the same functions for Ga-Ga-Ga and for As-As-As at $x = 0.5$.

The peaks in these distribution functions give hints about about the short-range bond-order in the liquids. For example, a peak near $\theta = 60^\circ$ corresponds to a relatively close-packed arrangement of the corresponding atomic group, with many nearest neighbors. In

contrast, a peak near 100° indicates a more tetrahedral structure, typical of covalent bonding. Thus, the upper part of Figs. 6 and 7 suggest that the Ga ions form a rather close-packed arrangement at $x = 0.8$ and $x = 0.5$, since there is a strong peak near 60° for both values of the cutoff r_c . By contrast, the lower parts of Figs. 6 and 7 suggest that, as expected, the As atoms have a more open arrangement at $x = 0.2$, since there are *two* peaks in g_3 at this concentration: a side peak near 50° , and another noticeable peak near 97° . We also observe the peak at 97° for As atoms at $x = 0.5$, however it is broader and less pronounced than at $x = 0.2$. In both Figs. 6 and 7, the Ga-Ga-Ga bond angle distribution depends little on r_c .

At $x = 0.2$, the As-As-As distributions show noticeable $50 - 60^\circ$ peaks only at the larger cutoff values. At the smaller cutoff radius, the $50 - 60^\circ$ peak is missing. Thus, at short distances, the As clusters tend to maintain the local version of the structure they have in the pure liquid phase (and the crystalline phase) which shows a strong peak at 97° , but at larger cutoffs the local structure differs from that of pure ℓ -As. We have made the same observation in connection with $g_{AsAs}(r)$ at the same concentrations, and with the shoulder in $S_{AsAs}(k)$. The 97° peak implies some tetrahedral order persisting to $x = 0.2$, though this peak is less pronounced than in pure ℓ -As [8].

We have also calculated the electronic properties of ℓ -Ga _{x} As _{$1-x$} . We calculate the single-particle electronic density of states $N(E)$ in the standard way, by using the expression

$$N(E) = \sum_{\mathbf{k}, E_{\mathbf{k}}} w_{\mathbf{k}} g(E - E_{\mathbf{k}}). \quad (3)$$

In this expression $E_{\mathbf{k}}$ denotes one of the energy eigenvalues of the single-particle wave functions at a particular \mathbf{k} point within the supercell Brillouin zone, $w_{\mathbf{k}}$ is the weight of that \mathbf{k} point (defined below), and $g(E)$ is a Gaussian smoothing function of width $\sigma = 0.2\text{eV}$. Our calculation is carried out by sampling the supercell Brillouin zone at eight special \mathbf{k} points, using the same choice of special points and weights as that of Holender *et al* in their calculations for pure ℓ -Ga [2], which have been well tested and found to be an adequate representation of the supercell Brillouin zone. This choice is, however, convenient rather than unique; we expect that other choice having the same number of \mathbf{k} points would have given

similar results, as has been found in pure ℓ -Ga. For each \mathbf{k} -point we include 40 conduction band states, and for each concentration, we obtain our final results by averaging over twelve representative liquid state configurations.

The resulting calculated density of states $N(E)$ is shown for the four concentrations $x = 0.2, 0.4, 0.6$, and 0.8 in Fig. 8. [We do not show our calculated $N(E)$ for $x = 0.5$, but it interpolates smoothly between $x = 0.4$ and $x = 0.6$.] As in our previous studies, the alloy has a clearly metallic density of states for all concentrations x . However, just as in our previous results for $\text{Ga}_x\text{Ge}_{1-x}$, the density of states becomes more and more free-electron like as the concentration x of the metallic component (Ga in this case) increases. Pure ℓ -As is semiconducting and has been calculated to have deep minima in the electronic density of states at the Fermi energy (E_F), and also at an energy of ~ -7 eV (measured from E_F) [8], which separates the s and p bands. Liquid Ga, on the other hand, has an almost free-electron like density of states. We see these features reflected in our simulations; as the figures indicate, the electronic density of states (DOS) has a pseudogap in the As rich phase which progressively fills up as the Ga concentration is increased, so that for $x = 0.8$ it is hardly noticeable. But even at low Ga concentration ($x = 0.2$), there is no minimum in the density of states at the Fermi energy. As for the pseudogap, we find that its position changes monotonically to lower energies (relative to E_F) with increasing Ga concentration. A similar pseudogap is reported in calculations for pure ℓ -Ge [9,29], for the same reason, i. e., a partial separation between s -like and p -like bands.

We have also computed the frequency-dependent electrical conductivity $\sigma(\omega)$ for $x = 0.2, 0.4, 0.5, 0.6$, and 0.8 , at frequencies ranging up to 2eV. $\sigma(\omega)$ is given by the standard Kubo-Greenwood expression [30]

$$\sigma(\omega) = \frac{2\pi e^2}{3m^2\omega\Omega} \sum_i \sum_j \sum_\alpha (f_j - f_i) |\langle \psi_i | \hat{p}_\alpha | \psi_j \rangle|^2 \delta(E_j - E_i - \hbar\omega). \quad (4)$$

where ψ_i and ψ_j are the single particle Kohn-Sham wave functions with Fermi occupancies f_i and f_j and energy eigenvalues E_i and E_j . Once again, we calculate the conductivity using the same set of eight special \mathbf{k} points used for $N(E)$, and averaging over the same

twelve representative ionic configurations, including 40 conducting band states for each \mathbf{k} . While there is some inaccuracy in using differences in Kohn-Sham eigenvalues, as we do in this equation, it is difficult to do better at present in liquid metals and semiconductors, and this same approach does give good agreement with experiment in a number of other liquid metals, especially at zero frequency but also for stoichiometric ℓ -GaAs [4] at finite frequencies.

The frequency-dependent conductivity is shown in Fig. 9 for $x = 0.2$ and $x = 0.8$, and its calculated zero-frequency limit is listed in Table I for the five concentrations $x = 0.2, 0.4, 0.5, 0.6$ and 0.8 , all at $T = 1600K$.

Several features of the conductivity graphs, and of the tabulated d. c. limits, deserve mention. First, the calculated value of the d. c. conductivity at $x = 0.5$ is very close to the experimental value: $0.84 \times 10^4 \text{ ohm}^{-1}\text{cm}^{-1}$, compared to the experimental value of $0.79 \times 10^4 \text{ ohm}^{-1}\text{cm}^{-1}$ [17]. Secondly, the conductivity has a weak minimum near $x = 0.5$. This is consistent with expectations based on second-order perturbation theory [31] which would predict that alloy scattering (due to concentration fluctuations) would be a *maximum* near $x = 0.5$. Thirdly, the frequency-dependence of $\sigma(\omega)$ becomes more metallic as x increases. Specifically, at $x = 0.8$, $\sigma(\omega)$ clearly decreases with increasing frequency, characteristic of a Drude metal, while for the highest As concentration ($x = 0.2$), the conductivity is nearly frequency-independent in the range of calculation. This behavior is closer to the nonmetallic behavior in which the conductivity *increases* with increasing frequency.

Finally, we have computed one important *atomic* transport coefficient, namely, the atomic self-diffusion coefficients D_{ii} for the majority species in the two liquids $\text{Ga}_{0.2}\text{As}_{0.8}$ and $\text{Ga}_{0.8}\text{As}_{0.2}$. In both cases, the D_{ii} 's can be extracted from a plot of the mean-square atomic displacement versus time, which approaches a straight line in the limit of large time. The expression is

$$D_{ii} = \lim_{t \rightarrow \infty} \frac{\langle |\mathbf{R}_i(t) - \mathbf{R}_i(0)|^2 \rangle}{6t}, \quad (5)$$

where $\mathbf{R}_i(t)$ denotes the position of an ion of species i at time t , and the triangular brackets

denote an average over all atoms of species i and over initial times. Plots of the mean-square atomic displacement as a function of time are shown in Fig. 10 for both types of atoms at $x = 0.2$ and 0.8 as indicated above; ζ From these we obtain $D_{Ga} = 2.1 \times 10^{-4} \text{ cm}^2/\text{sec}$ at $x = 0.8$; $D_{As} = 1.7 \times 10^{-4} \text{ cm}^2/\text{sec}$ at $x = 0.2$.

The value for D_{As} at $x = 0.2$ is about three times larger than that obtained by Li [8] for pure ℓ -As ($D \sim 0.6 \times 10^{-4} \text{ cm}^2/\text{sec}$). This difference is probably due to a combination of several factors. First, the calculations by Li are carried out at a temperature $\sim 450 \text{ K}$ lower than ours. Secondly, pure ℓ -As seems to have more covalent bonding than $\text{Ga}_{0.2}\text{As}_{0.8}$, which probably impedes atomic motion, giving a lower atomic diffusion coefficient for As. Thus, in short, this behavior seems to be consistent with the rest of our picture, which is that $\ell\text{-Ga}_x\text{As}_{1-x}$ rapidly acquires metallic conductivity, and corresponding structural properties for x as small as 0.2.

IV. DISCUSSION AND CONCLUSIONS

The most striking results of these calculations is that $\text{Ga}_x\text{As}_{1-x}$ remains metallic at all concentrations between $x = 0.2$ and $x = 0.8$, including the As rich value $x = 0.2$. Thus even low Ga concentrations are sufficient to render $\ell\text{-Ga}_x\text{As}_{1-x}$ metallic (recall that pure ℓ -As is semiconducting). This is reflected in the electronic density of states which shows no minimum at the Fermi energy for all concentrations studied. The liquid structure is also consistent with metallic behavior at all concentrations between $x = 0.2$ and 0.8 , although there are some clear deviations from the behavior seen in simple metallic alloys. Specifically, although the coordination number at all concentrations is larger than the value of four that might be expected in a predominantly covalent liquid, it is still smaller than that of a typical close-packed hard-sphere mixture. At $x = 0.2$ and 0.8 , the pair correlation functions and structure factors resemble those of the corresponding pure liquids, except that the split first peak in $S(k)$ of ℓ -As becomes a single peak with a weak shoulder in As.

It has been suggested [32] that semiconducting properties persist in a liquid only if the

liquid has the same short-range order as the crystalline phase. In the alloys we study, the liquid state has a short range order which is distinctly different from the solid. We also find that all these alloys are metallic, in agreement with the suggestion of Ref. [32]. By contrast, again in agreement with the picture advanced in [32], another compound semiconductor, stoichiometric CdTe, appears to preserve the crystalline short-range order, and also to retain its semiconducting characteristics in the liquid state. Such semiconducting behavior was indeed found in the *ab initio* calculation by Godlevsky *et al* [4]. It would be of interest to extend their calculations off stoichiometry, where metallic behavior is likely.

The other characteristics of ℓ -Ga _{x} As_{1- x} reflect its fundamentally liquid-metallic character. For example, the resistivity is predicted to exhibit typical Faber-Ziman behavior: a weak positive deviation from a linear concentration dependence near stoichiometry, which is caused by alloy scattering. The calculated values of the partial atomic diffusion coefficients are comparable to the diffusion coefficients of those other liquid semiconductors which are metallic in their liquid states. We find no evidence of a strong reduction in this value because of formation of clusters near stoichiometry; such cluster formation is not expected for Ga _{x} As_{1- x} because of the small electronegativity differences between the two species. One might speculate that, in other liquid semiconductors, such as stoichiometric ℓ -CdTe, which remain poorly conducting in the liquid state, the local structure is much more ionic near melting and the atomic diffusion coefficients are correspondingly lower.

In summary, our calculations show that Ga _{x} As_{1- x} is a reasonable metal at all concentrations between $x = 0.2$ and $x = 0.8$. In particular, there is no evidence of strong compound formation in the liquid state near $x = 0.5$. The electrical conductivity shows a concentration dependence typical of a liquid metallic alloy, with evidence of weak scattering from concentration fluctuations which reaches a maximum near $x = 0.5$. The electronic density of states shows no minimum at the Fermi energy; instead, it has a pseudogap between *s*-like and *p*-like occupied state which persists at all concentrations, though it is considerably weaker in the Ga-rich alloys. The atomic diffusion coefficient is calculated to be similar to that of other liquid semiconductors which are metallic in their liquid state. Finally, the liquid

structure shows some indications of deviation from the behavior of simple liquid metal alloys [25]. The principal evidence of deviation from behavior characteristic of a simple liquid alloy formation comes from the calculated pair correlation functions, structure factors, and bond angle distribution functions, all of which show some weak indications of departure from close-packed behavior: smaller coordination functions than in typical hard-sphere liquids, and a weak residue of tetrahedral bonding.

V. ACKNOWLEDGEMENTS

We are grateful for support by NASA, Division of Microgravity Sciences, under grants number NCC3-555 and NCC8-152. We also thank M. Scheffler and the research group at the Fritz-Haber Institute (Theory Department) for use of their *ab initio* code FHI96MD, and D. Matthiesen, A. Chait, and E. Almaas for many valuable conversations. These calculations were carried out using the SP2 at the Ohio Supercomputer Center and the RS/6000 cluster at the NASA Lewis Research Center.

REFERENCES

- [1] G. Kresse and J. Hafner, Phys. Rev. B **49**, 14251 (1994).
- [2] J. M. Holender, M. J. Gillan, M. C. Payne, A. Simpson, Phys. Rev. B **52**, 967 (1995).
- [3] F. Kirchhoff, J. M. Holender, and M. J. Gillan, Phys. Rev. B, **54**, 190 (1996).
- [4] V. V. Godlevsky, J. J. Derby, and J. R. Chelikowsky, Phys. Rev. Lett **81**, 4959 (1998); V. Godlevsky, J. R. Chelikowsky, J. Chem. Phys. **109**, 7312 (1998).
- [5] Q.-M. Zhang, G. Chiarotti, A. Selloni, R. Car, and M. Parrinello, Phys. Rev. B**42**, 5071 (1990).
- [6] R. Car and M. Parrinello, Phys. Rev. Lett. **35**, 2471 (1985).
- [7] R. Car and M. Parrinello, Phys. Rev. Lett. **60**, 204 (1988).
- [8] X. P. Li, Phys. Rev. **B41**, 8392 (1990).
- [9] R. V. Kulkarni, W. G. Aulbur, and D. Stroud, Phys. Rev. B **55**, 6896 (1997).
- [10] R. V. Kulkarni and D. Stroud, Phys. Rev. B**57**, 10476 (1998).
- [11] D. R. Hamann, Phys. Rev. B **40**, 2980 (1989); X. Gonze, R. Stumpf, and M. Scheffler, Phys. Rev. B. **44**, 8503 (1991)
- [12] L. Kleinman and D. M. Bylander, Phys. Rev. Lett. **48**, 1425 (1982).
- [13] J. P. Perdew and A. Zunger, Phys. Rev. B **47**, 558 (1993).
- [14] M. Bockstedte, A. Kley, and M. Scheffler, Comp. Phys. Communications **107**, 187 (1997).
- [15] R. Stumpf and M. Scheffler, Comp. Phys. Communications **79**, 447 (1994).
- [16] Of course 1600K is much closer to the melting point of stoichiometric GaAs and of pure As than it is to that of metallic Ga. Nontheless, a calculation at constant temperature

seems the best way to make uniform comparisons.

- [17] V. M. Glazov, S. N. Chizhevskaya, and N. N. Glagoleva, *Liquid Semiconductors* (Plenum, New York, 1969).
- [18] Vegard's Law may well be inaccurate for ℓ -Ga_xAs_{1-x}, but in the absence of experimental data for the concentration-dependence of the volume, it seems a reasonable interpolation.
- [19] S. Nosé, J. Chem. Phys. **81**, 511 (1984); W. G. Hoover, Phys. Rev. A **31**, 1695 (1985)
- [20] For the partial correlation functions $g_{ij}(r)$ and $S_{ij}(k)$, we use the standard definitions as given, for example, in Ref. ([24]) or Ref. ([25]).
- [21] J. P. Hansen, and I. R. McDonald, *Theory of Simple Liquids* (Academic Press, San Diego, 1991) p. 377
- [22] R. Bellissent, C. Bergman, R. Ceolin, and J. P. Gaspard, Phys. Rev. Lett. **59**, 661 (1987).
- [23] J. Hafner, Phys. Rev. Lett. **62**, 784 (1989).
- [24] Y. Waseda, *The Structure of Non-Crystalline Materials, Liquids, and Amorphous Solids* (McGraw-Hill, New York, 1980).
- [25] N. W. Ashcroft and D. Stroud, Solid State Physics **33**, 1 (1978).
- [26] M. C. Bellissent-Funel, P. Chieux, D. Levesque, and J. J. Weis, Phys. Rev. A. **39**, 6310 (1989)
- [27] C. Bergman, C. Bichara, P. Chieux, and J. P. Gaspard, J. Phys. Colloq. bf C8-46, 97 (1985)
- [28] N. W. Ashcroft and D. C. Langreth, Phys. Rev. **156**, 695 (1967).
- [29] W. Jank and J. Hafner, Europhys. Letters, **7**, 623 (1988).
- [30] D. J. Thouless, Phys. Rep. **13**, 93 (1974).

[31] See, for example, T. E. Faber, *Introduction to the Theory of Liquid Metals* (Cambridge U. P., 1972).

[32] A. Joffe and A. Regel, *Progress in Semiconductors* (Heywood, London, 1960), Vol. 4, p. 237.

TABLES

TABLE I. D. c. conductivity at the five concentrations, obtained by extrapolating low frequency
a. c. conductivity results.

Concentration (%)	20	40	50	60	80
σ_{dc} (10^4 ohm $^{-1}$ cm $^{-1}$)	0.93	0.9	0.84	0.91	1.1

FIGURE CAPTIONS

1. (a) Pair correlation functions $g_{GaGa}(r)$, $g_{AsAs}(r)$, and $g_{GaAs}(r)$ for ℓ -Ga_xAs_{1-x} at a temperature of 1600 K and concentration $x = 0.5$. The graphs are vertically offset by one unit each for clarity.
2. (top) $g_{GaGa}(r)$ for $x = 0.8$; (bottom) $g_{AsAs}(r)$ at $x = 0.2$ and $T = 1600$ K.
3. Full line: Calculated neutron structure factor $S(k) = \sum_{i,j=Ga}^{As} f_{ij}(k) S_{ij}(k)$, where $f_{ij}(k)$ is the neutron form factor, for $x = 0.5$. Open circles: measured $S(k)$ as obtained by neutron diffraction [ref. [27]].
4. Partial structure factors $S_{GaGa}(k)$, $S_{AsAs}(k)$, and $S_{GaAs}(k)$ for $x = 0.5$. $S_{AsAs}(k)$ is vertically offset for clarity.
5. Calculated partial structure factors (top) $S_{GaGa}(k)$ at $x = 0.8$; (bottom) $S_{AsAs}(k)$ at $x = 0.2$.
6. Calculated bond angle distribution functions $g(\theta, r_c)$ for (top) groups of three Ga atoms at a concentration $x = 0.8$, and (bottom) groups of three As atoms at a concentration $x = 0.2$, both for two different cutoff radii, $r_c = 3.4\text{\AA}$ and $r_c = 3.8\text{\AA}$, as defined in the text.
7. Same as for Fig. 6 but for $x = 0.5$ and (top) $g_{GaGaGa}(\theta, r_c)$; (bottom) $g_{AsAsAs}(\theta, r_c)$;
8. Single-particle electronic density of states $N(E)$ for Ga_xAs_{1-x} at $x = 0.2, 0.4, 0.6$, and 0.8 . The Fermi energy in each case is shown as a dashed vertical line.
9. Calculated electrical conductivity $\sigma(\omega)$ for Ga_xAs_{1-x} at $x = 0.2$ and $x = 0.8$.
10. Calculated mean-square displacement $\langle |\mathbf{R}_i(0) - \mathbf{R}_i(t)|^2 \rangle$, plotted as a function of t at $x = 0.2$ for As and at $x = 0.8$ for Ga.

FIGURES

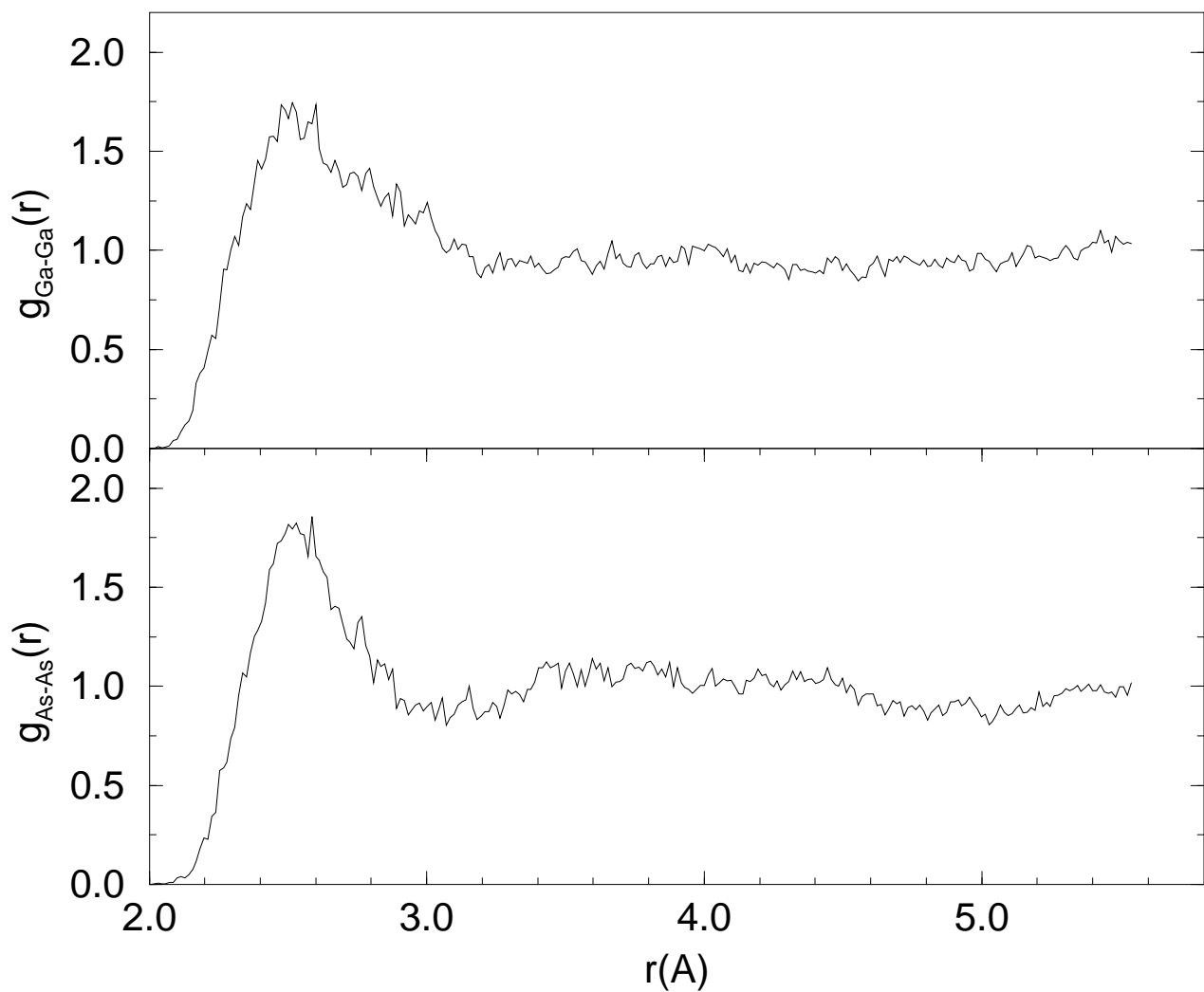


FIG. 1.

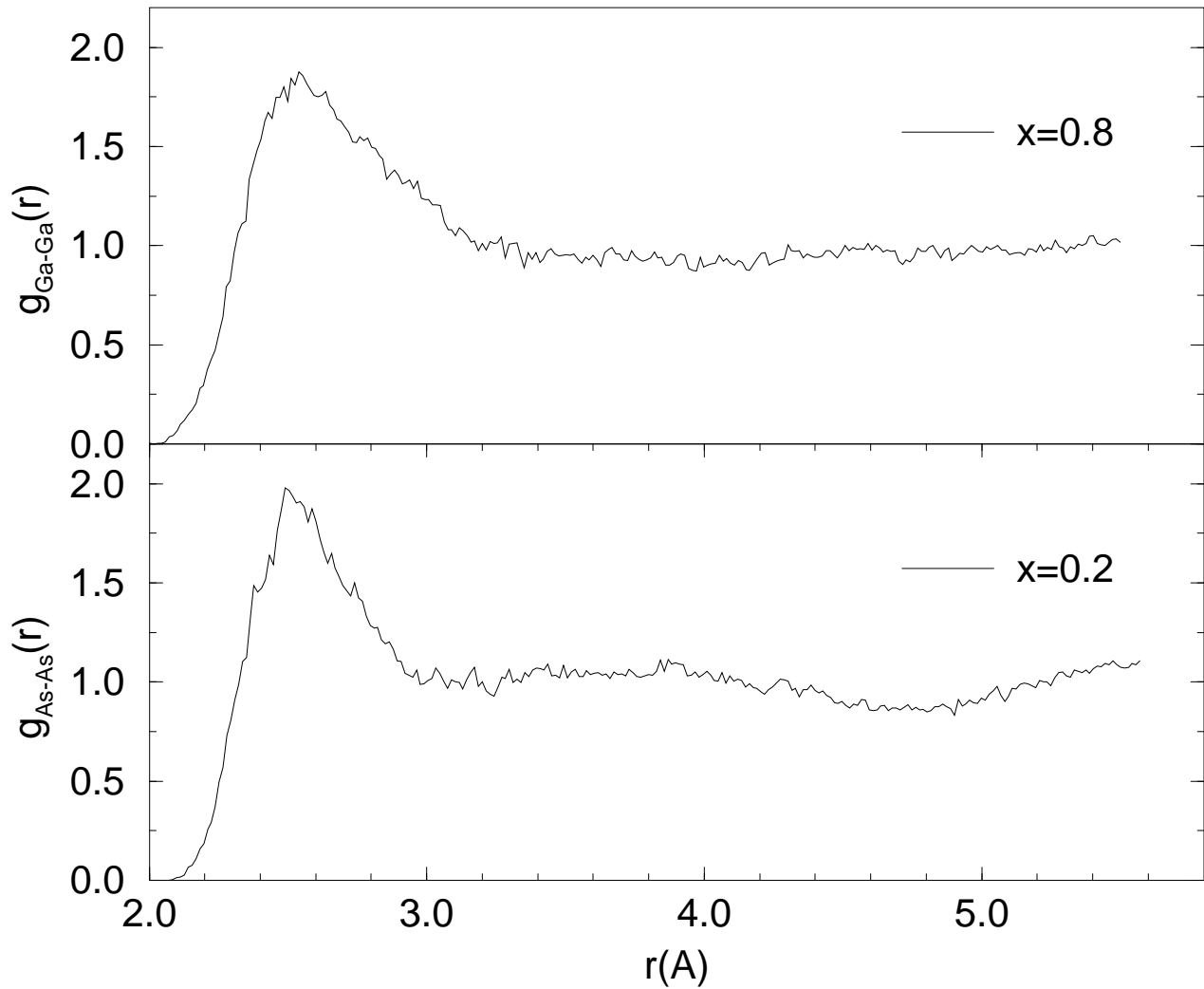


FIG. 2.

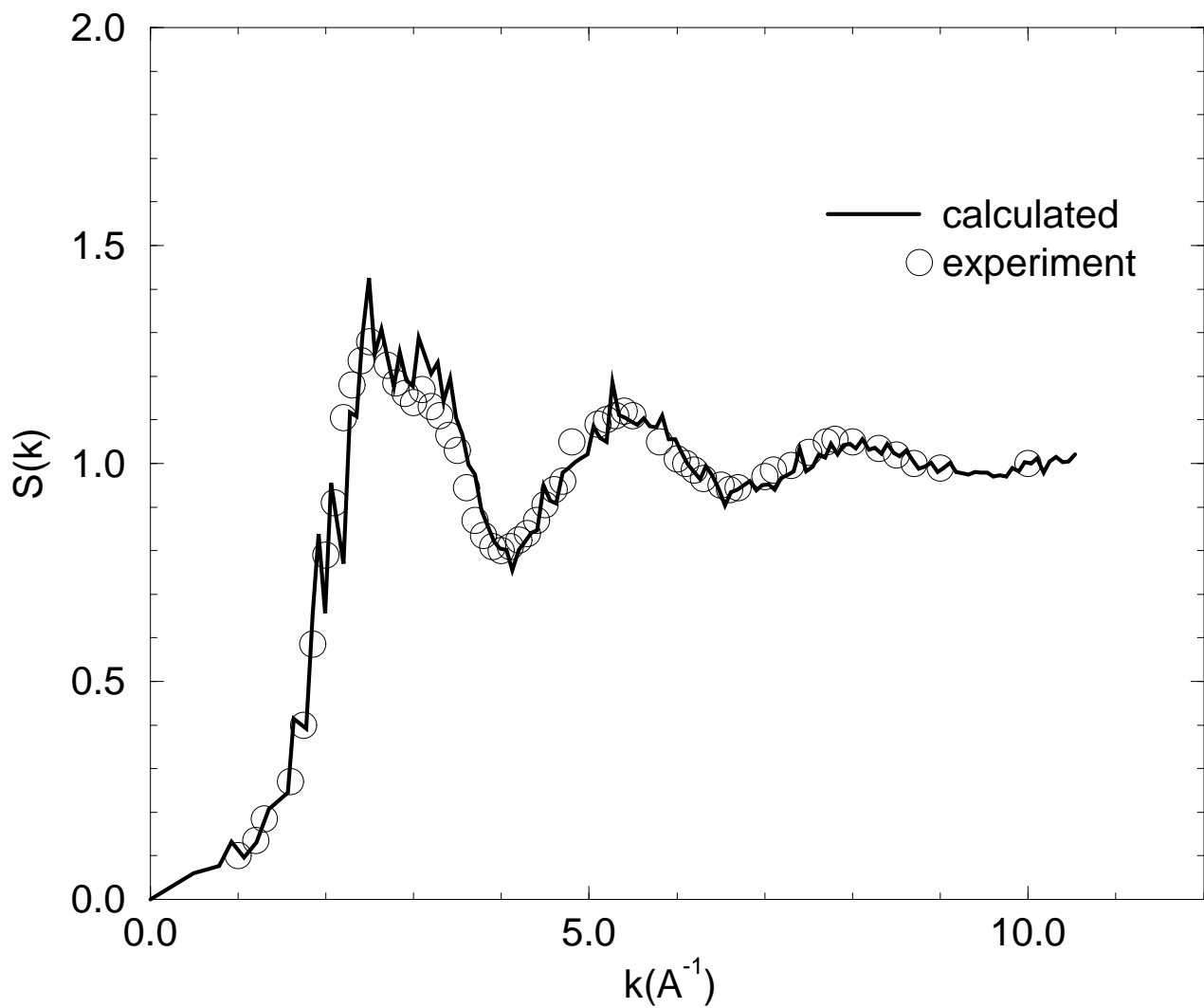


FIG. 3.

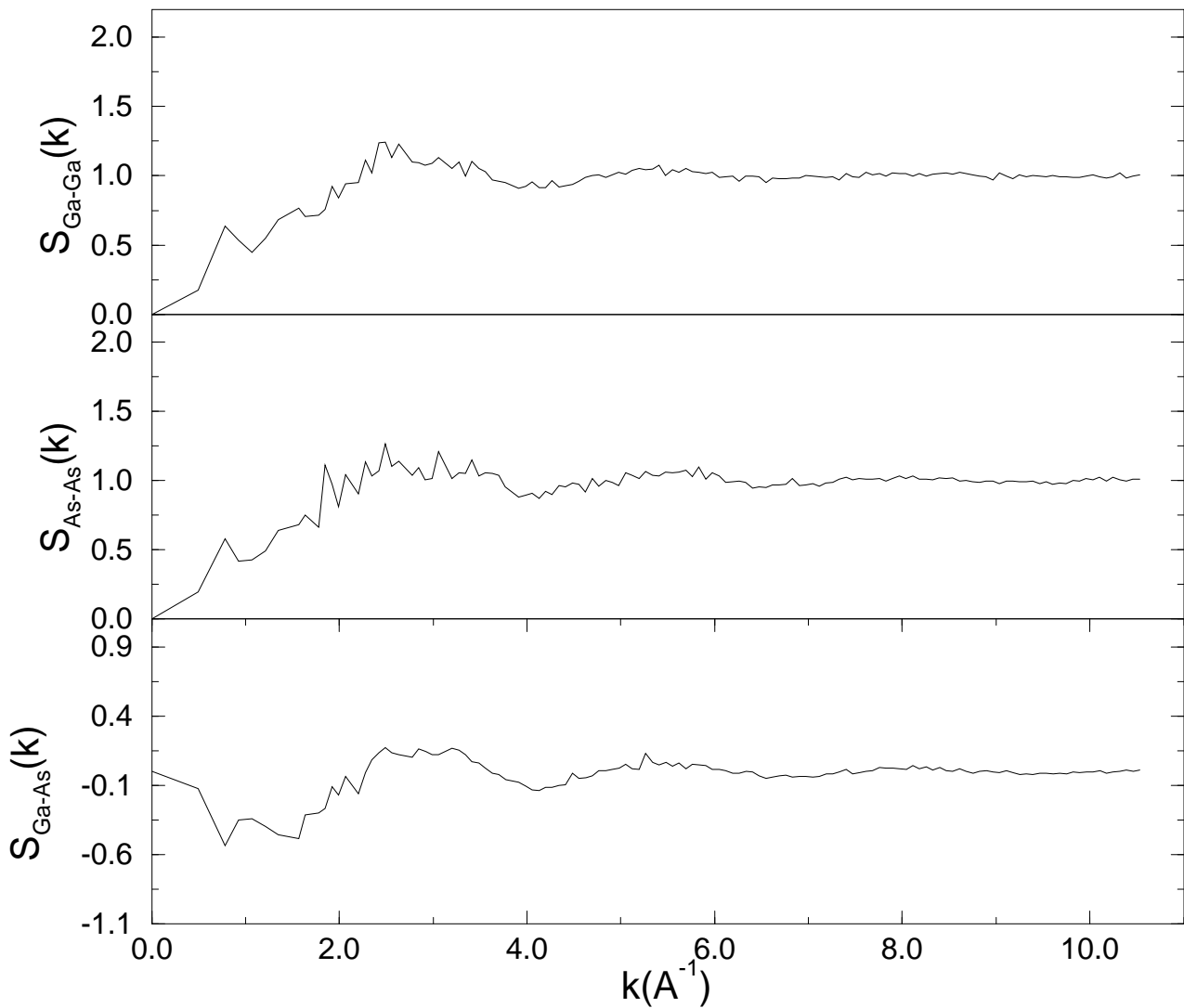


FIG. 4.

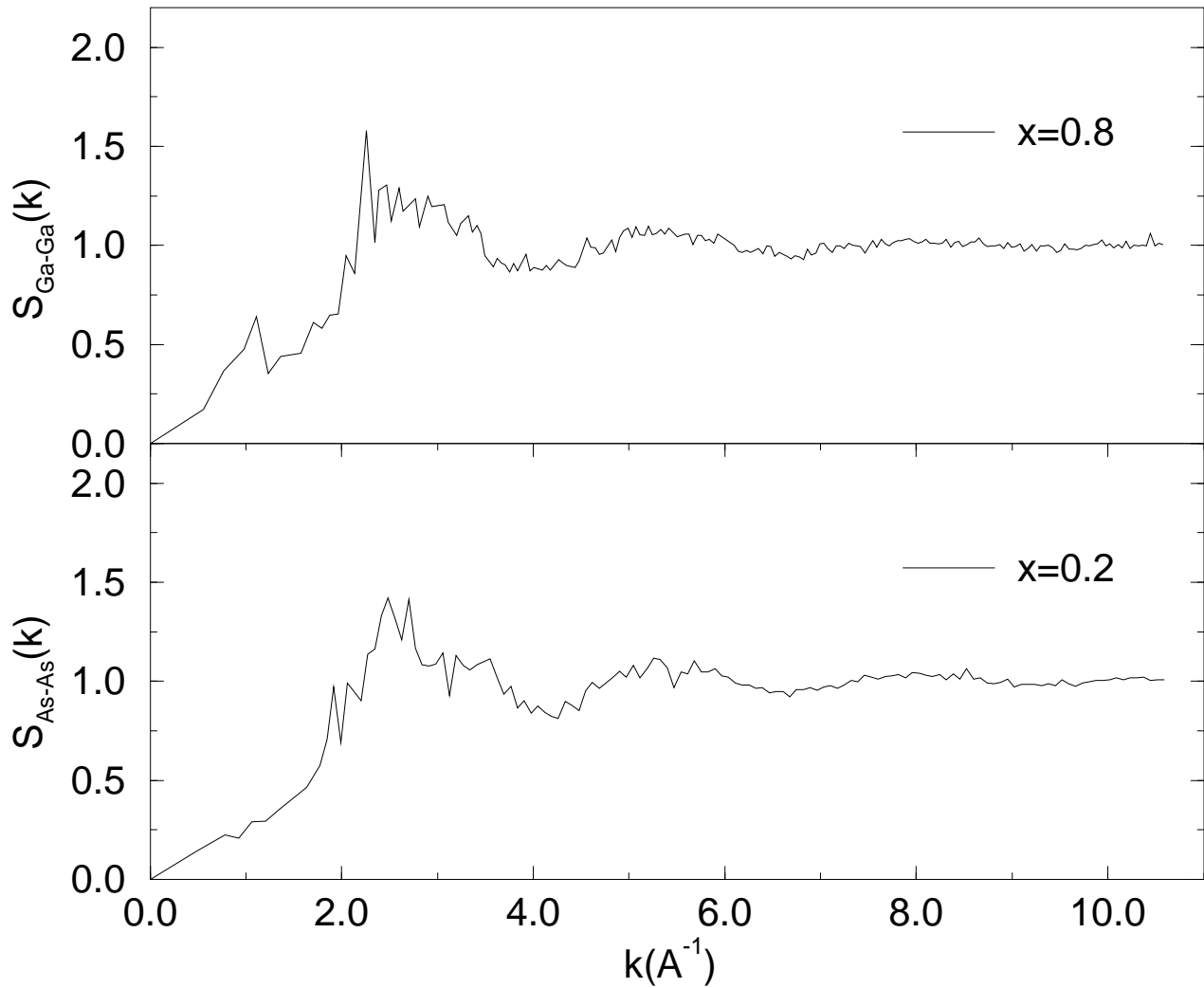


FIG. 5.

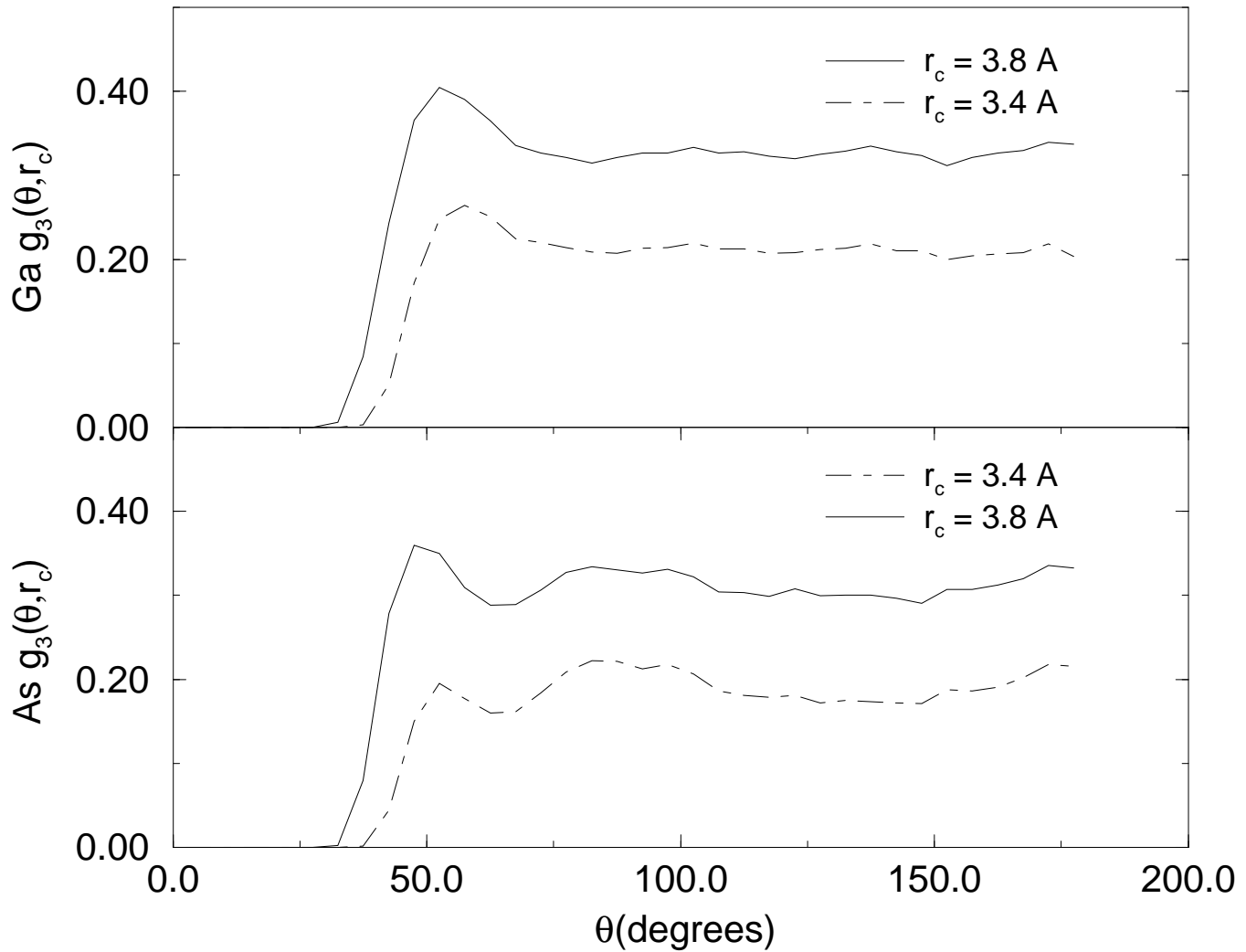


FIG. 6.

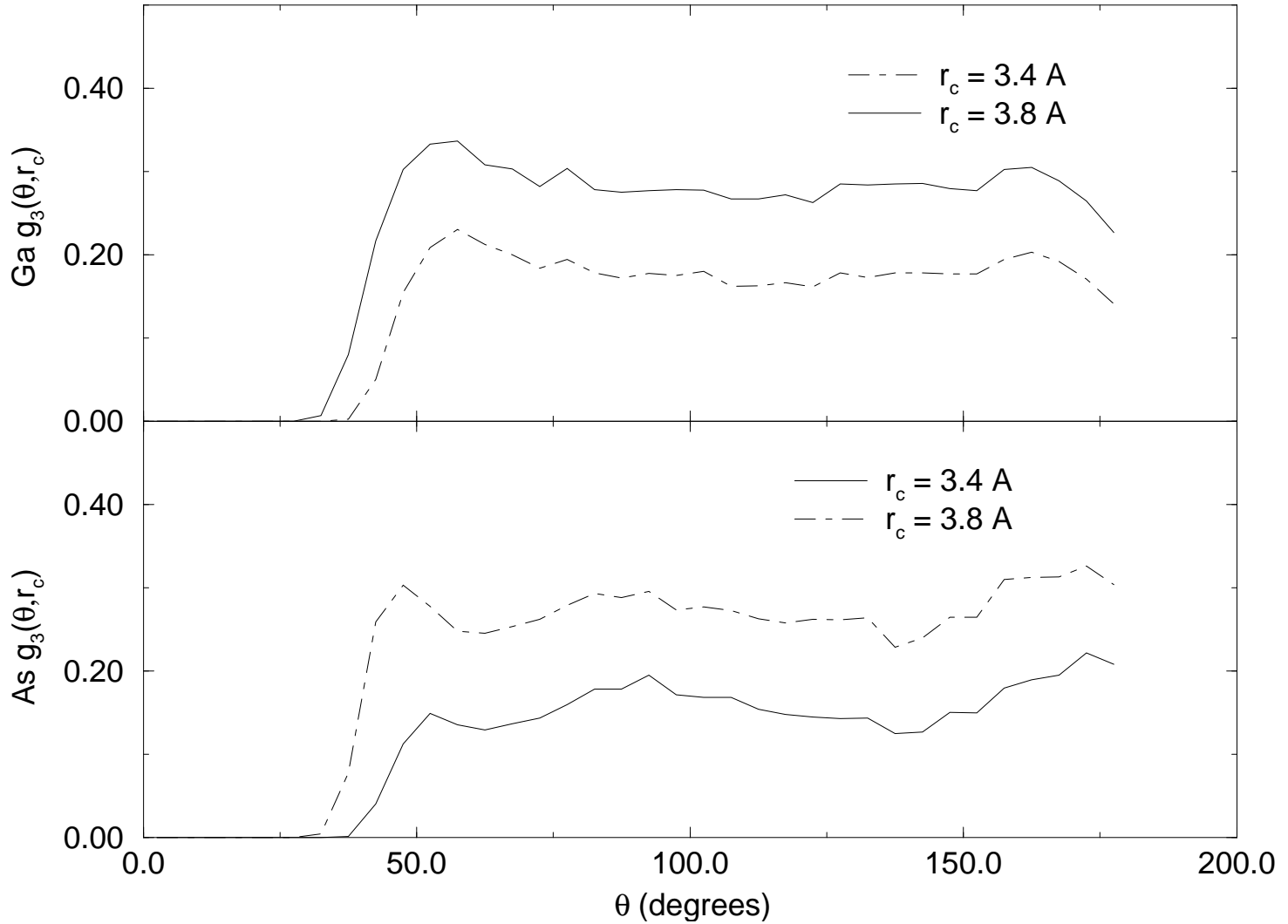


FIG. 7.

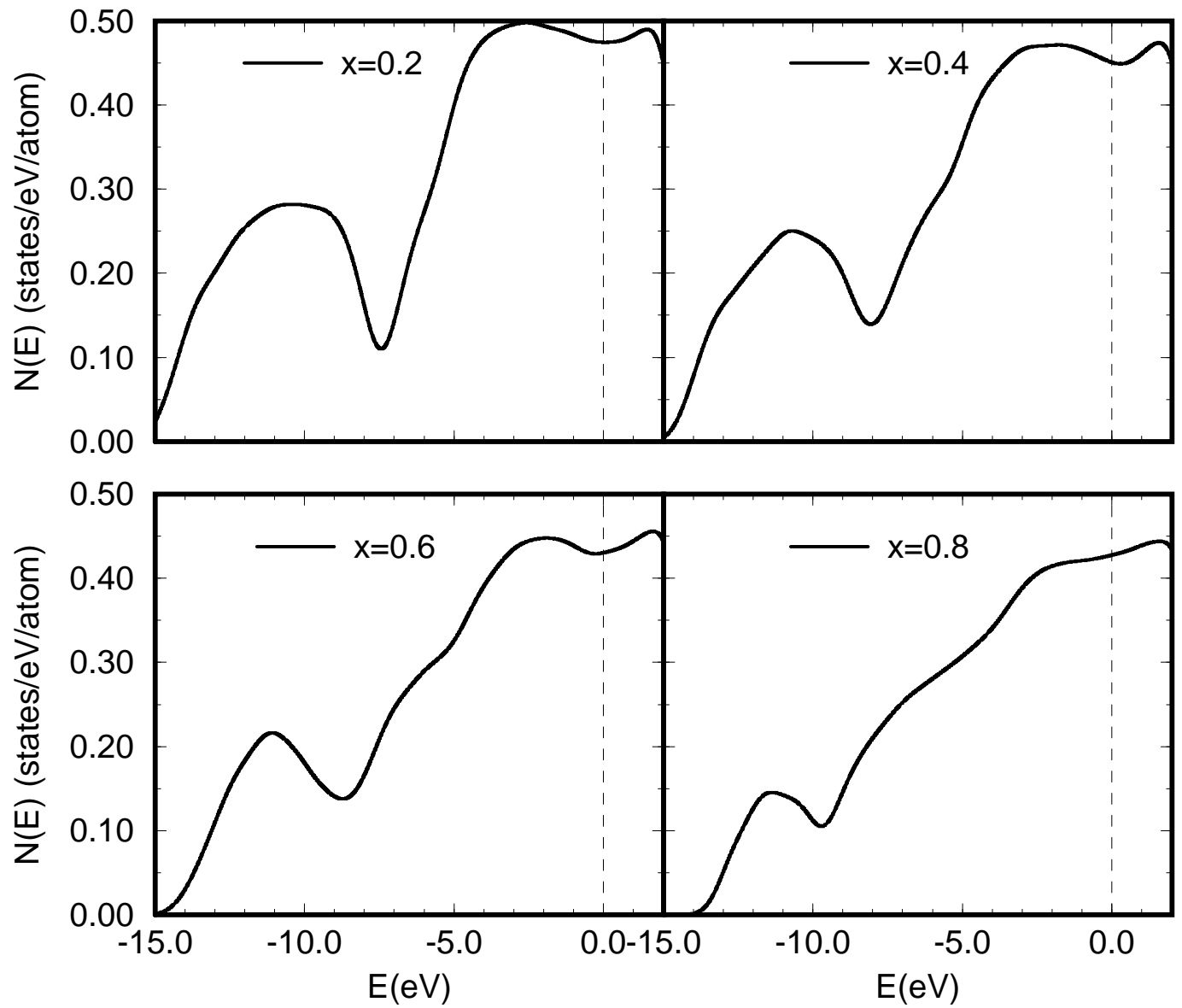


FIG. 8.

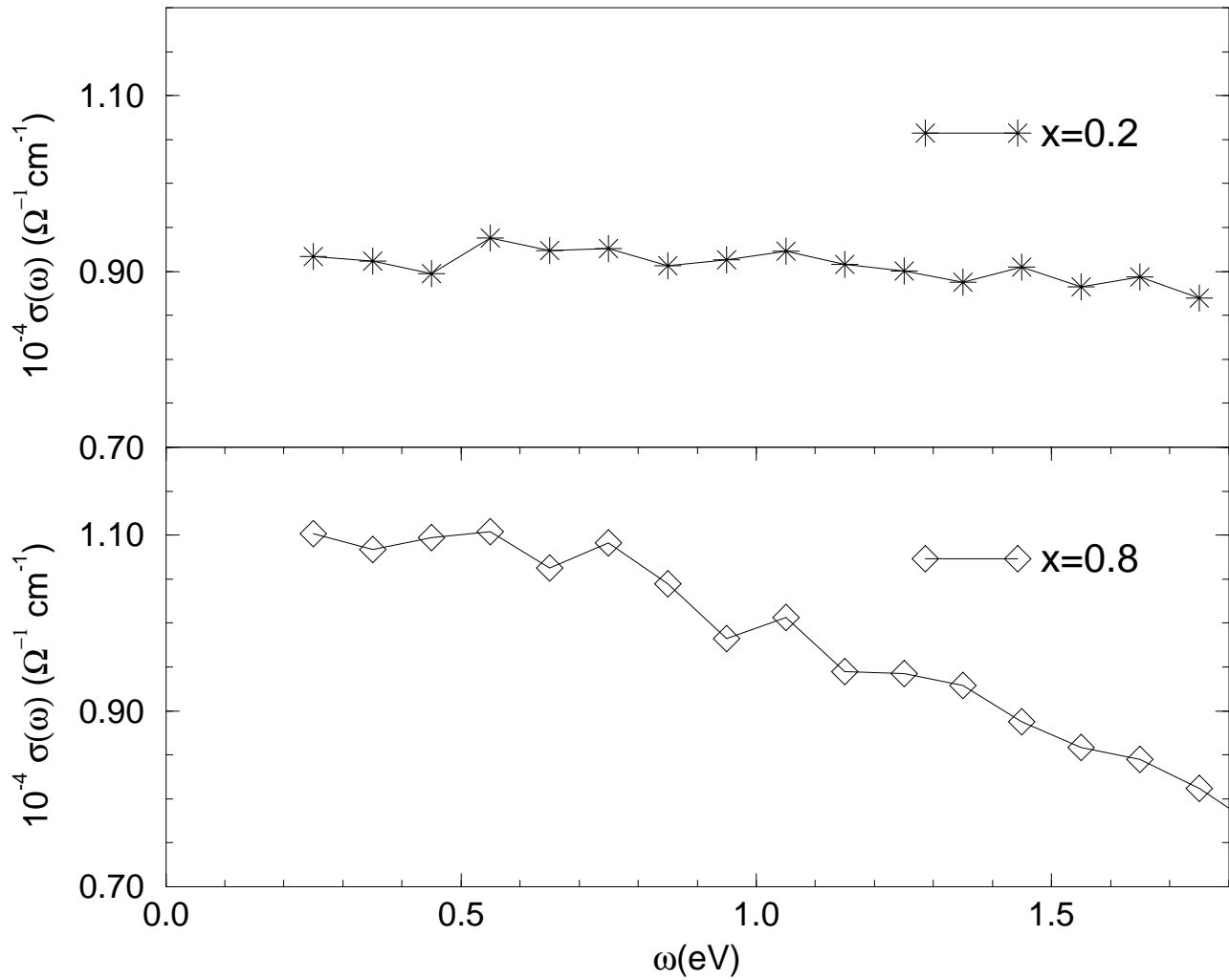


FIG. 9.

Mean Square displacement

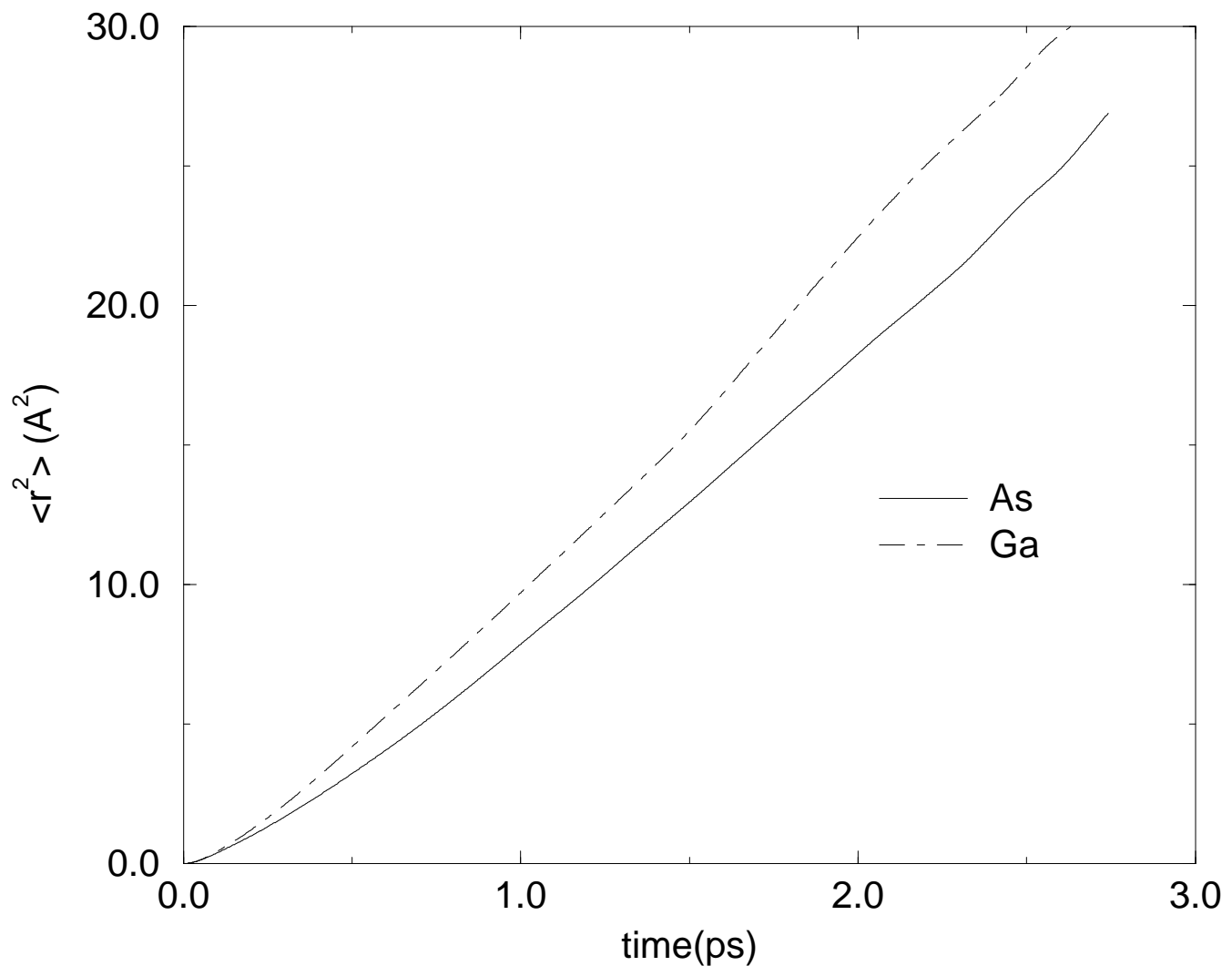


FIG. 10.